DOI: 10.37190/ ABB-02489-2024-02

A Study on the Performance of WordSID Thorax Module for Thorax Injury Prediction in e-Bike Rider Based on Real Accident Data

Yi Chang[1], Yongcheng Long[1], Xinming Wan[1*], Yu Liu[1], Guojie Wang[1], Guanjun Zhang[2], Zhi Xiao[2]

[1]China Automotive Engineering Research Institute Co., Ltd. Chongqing, China

[2]College of Mechanical and Vehicle Engineering, Hunan University, Changsha, China

[*]Corresponding author: Xinming Wan, China Automotive Engineering Research Institute Co., Ltd. Chongqing, China, e-mail address: wanxm_2006@163.com

Submitted: 25th July 2024

Accepted: 26th October 2024

Abstract In this study, the analysis of 2824 vulnerable road users (VRU) accident data from China's FASS (Future mobile traffic Accident Scenario Study) database indicates that VRU side impacts are the most common collision scenarios. A typical accident (minivan-to-eBike) from the FASS database was selected for accident reconstruction. WordSID thorax module has been employed to evaluate e-Bike Rider thorax injuries and its kinematic difference has been investigated as well. The e-Bike Rider was simulated by THUMS (Total Human Model for Safety). The kinematic data of THUMS thorax obtained from the accident reconstruction were used as the boundary conditions of WorldSID dummy thorax to simulate the collision between thorax and accident vehicle, and the deflection of WorldSID dummy thorax was outputted and compared with THUMS rib deflection. The accident reconstruction results using the THUMS model match the human thorax injury conditions. The WorldSID thorax module can effectively replicate the motion of the thorax and predict thorax injury conditions in the minivan-to-eBike collision, but it does not reflect the bending of the spine during the e-Bike Rider impact process, nor does it consider the impact of forces on the head, neck, and lower limbs. Therefore, further improvements are still necessary.

Keywords e-Bike Rider injury, minivan to e-Bike collision, accident reconstruction, WordSID thorax module.

I. INTRODUCTION

According to the 2023 Global Status Report on Road Safety, in 2021, 1.19 million people died in road traffic accidents, with pedestrians accounting for 23% and two/three-wheeled vehicle users accounting for 27% [20]. In China, according to the “Annual Statistical Report of Road Traffic Accidents 2020”, the number of fatalities from road traffic accidents was 61,703 with pedestrians making up 28.3% and two/three-wheeled vehicle users 46.8% (e-Bike drivers accounted for 13.5%) [1].

Thorax injury mechanisms for cyclists, as opposed to vehicle occupants, are not yet clear. Currently, among all NCAPs, those with relatively comprehensive VRU safety protection test projects include Euro-NCAP, J-NCAP, A-NCAP, K-NCAP, C-NCAP, and Latin-NCAP. Considering variations in actual road and traffic conditions in countries and regions, there is a big number of VRU safety protection evaluation, including head and leg protection, while there are only a few evaluations for thorax protection. But for VRUs, thorax injuries are the second most fatal type of injury after head injuries [10], [15], [21], [23], Therefore, the study of thorax impactors becomes very necessary. Several studies have chosen side impact dummies to assess thorax injuries in VRUs. Following experiments, Fredriksson et al. reported that the thorax of side impact dummies with good biofidelity can be used to evaluate models with higher hoods, such as SUVs [6]. In the European SENIORS (Safety-ENhancing Innovations for Older Road userS) project, a thorax injury prediction tool (TIPT) was developed and evaluated through the separated ES-2 dummy thorax finite element model, but its biofidelity was relatively low [25], [26]. Saraç Karadeniz et al. from Turkey designed a thorax impactor, ThImp-PED, applicable to SUV and LTV (light tactical vehicle) models based on the thorax structure of the ES-2 dummy, which passed the corresponding thorax calibration procedures. The test results from bus collisions also showed that the impactor performed well [9]. However, since the mechanisms of VRU thorax injuries and evaluation indicators are not yet clear, there is currently no practical application of thorax impactors in VRU thorax evaluation.

THUMS model can be used to assess the load conditions of occupants and pedestrians under different scenarios [8], [16], [18] and can also be used for kinematic research and injury prediction of cyclists [17]. However, current research on VRU thorax injuries mainly focuses on pedestrian injuries. For example, Han et al. selected THUMS finite element model to analyse the thorax dynamic response of pedestrians in collisions, concluded that the risk of rib injuries for pedestrians is higher in minivan collisions [7]. Li Guibing et al. reported the reconstruction of a collision accident between a minivan and a pedestrian based on the THUMS model. Research results indicated that THUMS has a good capability in predicting pedestrian thorax injuries observed in the real world and it was noted that rib fractures and lung compression on the struck side were mainly caused by deflection of the lower ribs [11]. But there is relatively little research on thorax injuries of e-Bike Riders. Hence, it is necessary to understand thorax injury mechanisms that will allow for the development of protection measures for e-Bike Riders.

Considering that rib fractures are determined by the amount of thorax deflection [24], and that injury criteria based on thorax deflection are better in predicting thorax injuries than those based on acceleration and force [2], the use of the WorldSID thorax module to simulate the collision between the thorax of the e-Bike Rider and the minivan was given priority.

In this study, the accident data of VRU in China are analyzed, obtained the probability distribution of VRU accident scenarios, selected a typical case, and used the THUMS model for accident reconstruction. The initial position of the THUMS thorax collision and the kinematic parameters of T8 (8th thoracic vertebra) obtained from the accident reconstruction were used as the initial position and boundary conditions for the WorldSID thorax module to simulate the collision between the WorldSID thorax and the accident vehicle. The response differences between the WorldSID thorax and the THUMS model thorax were compared. Although the effectiveness of the WorldSID in occupant conditions has been verified, its biofidelity in VRU complex conditions is still unclear. Therefore, the results of this study can provide a reference for the feasibility of using the WorldSID thorax module to assess VRU thorax injuries.

II. METHODS

Source of Accident Data

The FASS (Future mobile traffic Accident Scenario Study) database was established by China Automotive Engineering Research Institute Co., Ltd. (CAERI), in order to obtain traffic accident-related data to support vehicle traffic safety analysis and evaluation [3], [4], [12]. The accident investigation focuses on on-site investigation combined with accident tracking, and each in-depth investigation case includes data on people, vehicles, roads, and the environment, covering data before, during, and after the collision, totaling 46 survey forms and over 3,700 fields. The database uses the Abbreviated Injury Scale (AIS) 2005 for injury classification.

Accident Case Selection

This study analyzed the scenarios of 2824 VRU accidents from 2018 to 2022 in the FASS database,The case screening process is shown in Figure 1.

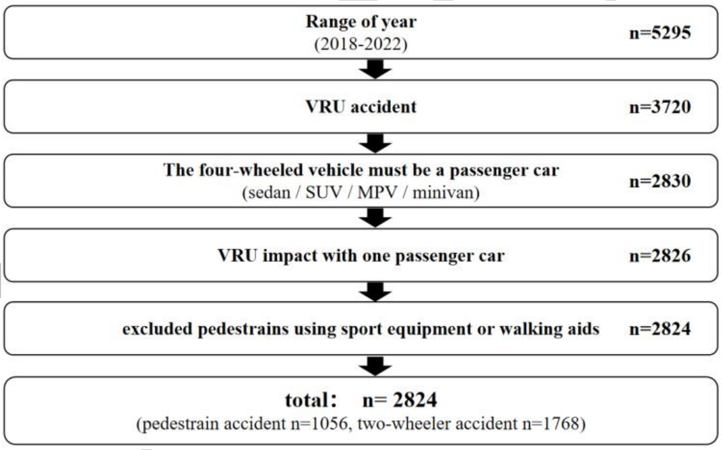

Fig. 1. case screening process

The definition of the accident scene is based on the behavior of the VRU before the accident. A statistical analysis of the collision scenarios in the aforementioned VRU accidents revealed that side impacts of VRUs are the most common, as shown in Table 1. type of accident (UTYP) is a field in the FASS database that describes the scenario of accident. It is found that in collisions between VRU and minivans, thorax injuries to VRUs are significantly higher than in collisions with sedans and SUVs [7]. Therefore, this paper selected a minivan-to-eBike collision accident from a relatively high proportion of scenarios (UTYP 301). In this accident the e-Bike rider suffered at least one rib fracture in the thorax, as one of the purposes of this study is to compare the injuries based on THUMS with those recorded in the FASS accident data.

TABLE 1
VRU ACCIDENT UTYP TOP3

Pedestrian Accident* *N=1056(37.4%)*		Two/Three-Wheeler Accident N=1768(62.6%)	
UTYP	Proportion	*UTYP*	Proportion
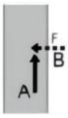 421	27.2%	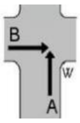 301	10.5%
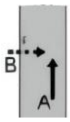 401	22.8%	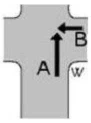 321	8.2%
 671	6.7%	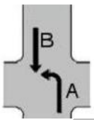 211	6.2%
total	67.0%	total	24.9%

*The dashed Arrow represent pedestrian

The collision conditions of this case were determined based on the on-site surveillance video and accident investigation results, showed in Figure 2. In this case, the e-Bike rider moved from the driver's side (left front) to the co-pilot side (right front) of the minivan. The minivan was traveling at approximately 30 km/h without significant deceleration, while the e-Bike decelerated before the collision and had almost stopped at the moment of impact. The impact trace of the vehicle was determined by vehicle survey. The video showed that the right side of the e-Bike rider's thorax only collided with the vehicle, making no contact with the ground, as shown in Figure 3. This evidence, combined with the rib fracture on the right side, suggested that the vehicle was the cause of the e-Bike rider's thorax injury.

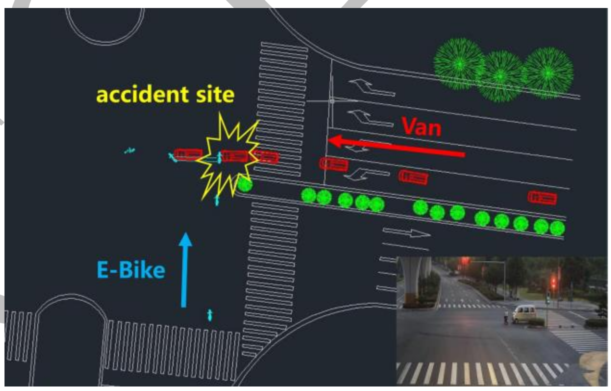

Fig. 2. Sketch and video

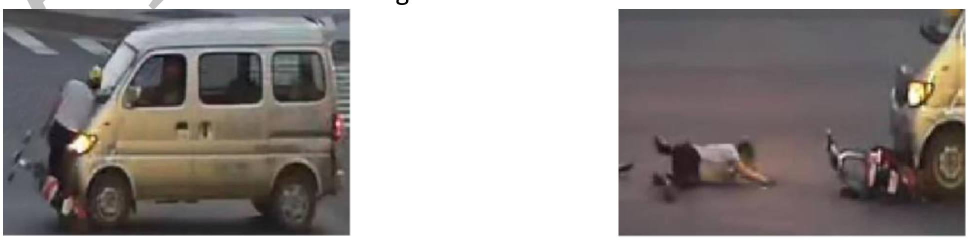
(a) (b)

Fig. 3. e-Bike rider's's thorax collision
(a. right thoraxt in contact with the hood; b. left thorax in contact with the ground)

Simulations of Car to VRU Impact

A minivan model of similar dimensions was selected for accident reconstruction[19]. Table 2 recorded its front-end size. The model was simplified while retaining the vehicle's kinematic and dynamic characteristics to reduce the complexity of the vehicle, with the finite element model was shown in Figure 4.a. The e-bike model was reconstructed according to the dimensions recorded in the FASS file - the dimensions are illustrated in Figure 4.b. The THUMS V402 model was used to simulate the e-Bike rider's and was positioned based on the initial collision position between the minivan and the e-Bike rider's which was extracted from the collision video.

TABLE 2
COMPARISON OF FASS INFORMATION AND FE MODEL

Car type	Mass[kg]	H1[cm]	H2[cm]	H3[cm]	L1[cm]	L2[cm]	L3[cm]
FASS_minivan	1020	62	75	119	3	32	43
Model_minivan	1026	55	79	117	5	34	62
FASS_e-Bike	55	73	99	-	50	100	-
Model_e-Bike	55	73	101	-	52	105	-

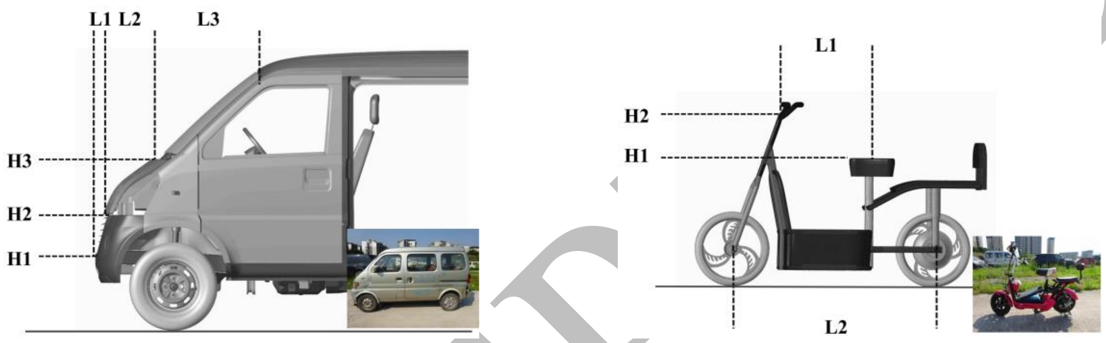

(a) (b)

Fig. 4. Accident vehicle and its finite element model (**a**. minivan; **b**. e-Bike)

Table 3 shows the basic information and thorax injury information of the e-Bike rider in the accident; the injuries were obtained from the hospital's medical records.

TABLE 3
BASIC INFORMATION AND THORAX INJURY INFORMATION OF THE E-BIKE RIDER

	Weight [kg]	Standing height [cm]	Sitting height [cm]	Age	Gender	Thorax injury
e-Bike rider	70	175	94*	66	Male	1）Multiple rib fractures on the right side (AIS 2) 2）Pulmonary contusion (AIS 3)
THUMS	77	175	89	-	Male	-

*This size refers to "Human dimensions of Chinese adults" from Chinese national standard (GB/T 10000-2023).

The accident was reconstructed according to the collision conditions and the definitions of the global coordinate system; Y-Offset, vehicle collision angle, speed, and other parameters are exhibited in Figure 5. The centre of mass of the THUMS head was determined to be 154 mm away from the vehicle's longitudinal axis. Based on the video, the collision speed of the minivan was set at 30 km/h, and because the speed of the e-Bike was lower, it was set to 0 km/h in the simulation. The collision angle was set at 90 degrees, between the vehicle's lateral center plane and the e-Bike rider's lateral center plane.

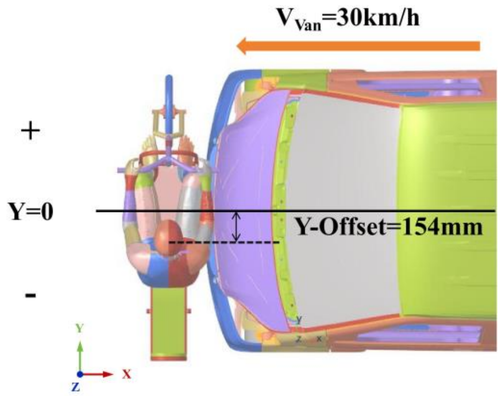

Fig. 5. Definition of vehicle Y-Offset and velocity

Local coordinate systems were defined at the THUMS T1 to T10 vertebrae, and the deflection of the point with the greatest deformation of each rib relative to its corresponding vertebra in the X direction was output(Figure 6.a). For comparison, the deflection at the outermost point of the ribs was also output(Figure 6.b).

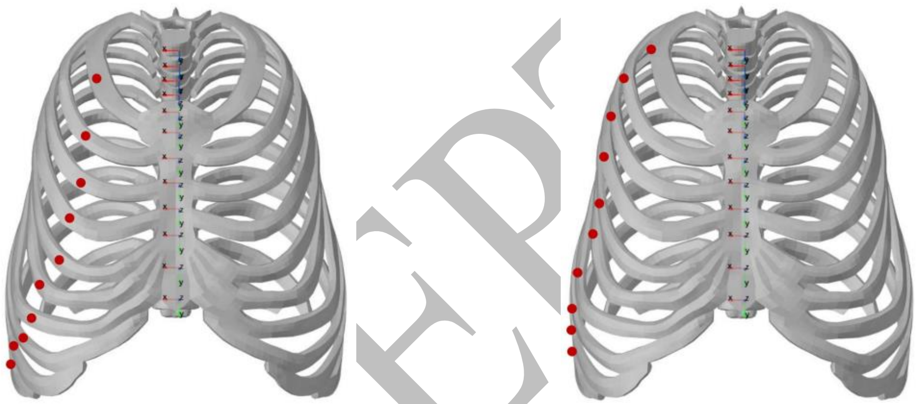

(a) (b)

Fig. 6. THUMS rib deflection measurement point(a. Maximum; b. Outermost)

Simulations of WordSID Thorax Module

According to the definition of thorax height by McConvile et al. [13], the thorax height of THUMS is about 344mm. Therefore, we have retained a torso of similar height for the WorldSID dummy (about 358mm). This module includes the arms, thorax, and part of the abdomen, with a total weight of 14.97 kg. The WorldSID thorax module was separated, and the T8 acceleration sensor was aligned with the T8 position of the THUMS. The position of the WordSID thorax module was adjusted to match the e-Bike rider's thorax segment, and the arm angles were aligned with the e-Bike rider's arms, as depicted in the final relative position in Figure 7. The initial position of the THUMS thorax collision and the initial velocity of the T8, which were obtained from the accident reconstruction were used as the initial position and boundary conditions for the WordSID thorax module to simulate the collision between the WorldSID dummy's thorax (Y-Offset_T8=332mm) and the accident vehicle (0km/h). Secondly, in order to study the effect of abdominal mass on the motion and deflection of the thorax module, the abdominal mass (12kg) suggested by Zander et al. [26] was added to T12, and the deflection of the WordSID thorax module (including with the added abdominal mass and without the added abdominal mass) was finally output and compared with the rib deflection of THUMS.

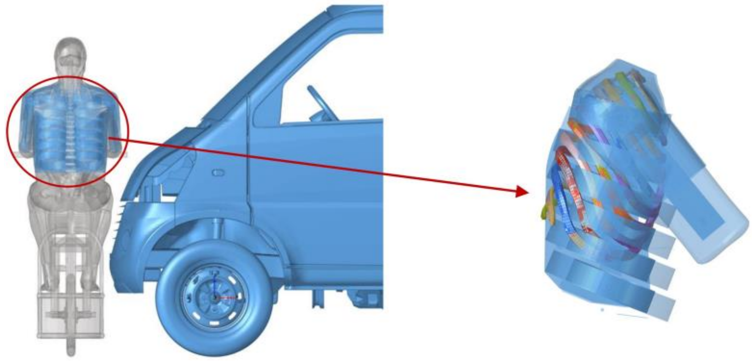

(a) (b)

Fig. 7. Simulation Settings (a. WorldSID thorax module Position Setting; b. Relative Position)

III. RESULTS

Accident Reconstruction Results

The whole-body kinematics of the e-Bike rider are shown in Figure 8, with a total simulation time of 200ms and an interval of 40ms between each image. The moment before the e-Bike contact with the minivan is at 0ms. The e-Bike rider's legs and hips are first in contact with the minivan. At approximately 30ms, the lower thorax begins to contact the vehicle's hood, and at 80ms, the thorax starts to enter the rebound stage. At 100ms, the head makes contact with the windshield, and at 120ms, the thorax leaves the hood.

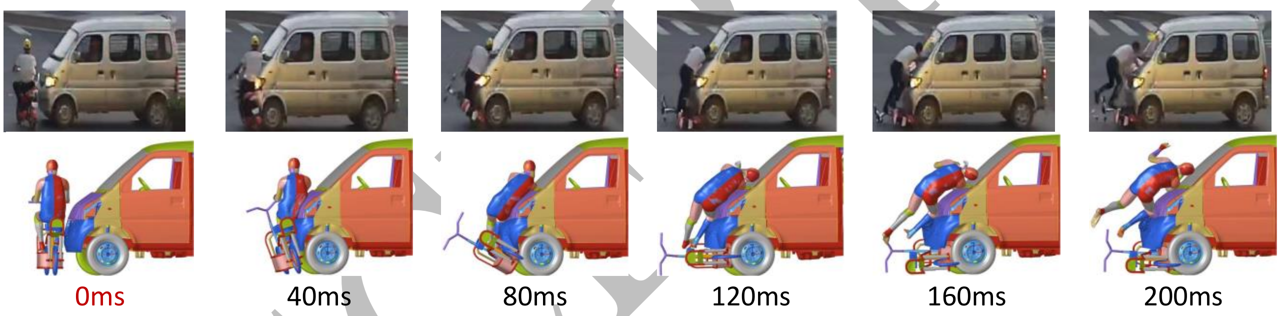

Fig. 8. Comparison of accident video and reconstruction results

Combined with the investigation of the accident vehicle, the vehicle traces were compared with the deformation of the vehicle model in the simulation. The vehicle model's bumper, hood, and windshield all showed significant deformation (Figure 9.b), which matched the collision traces of the accident vehicle (Figure 9.a).

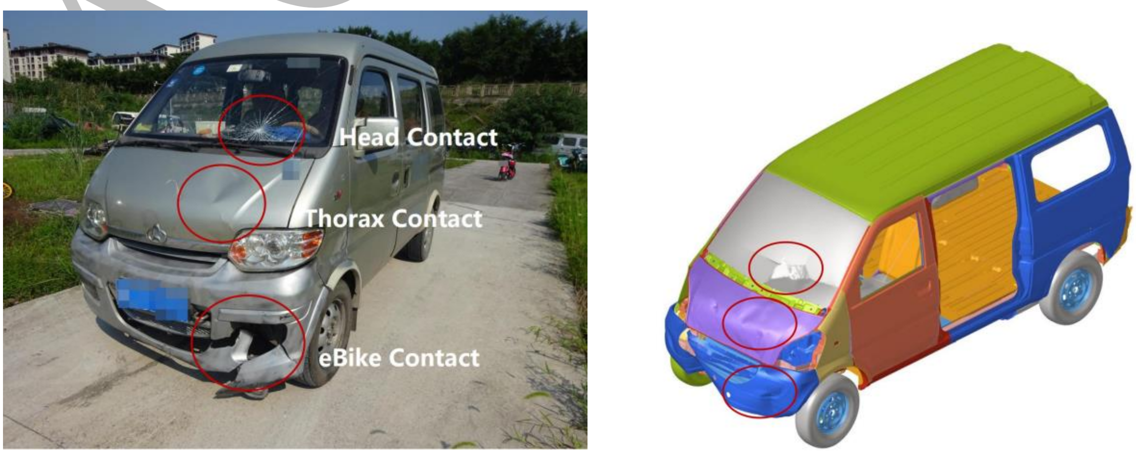

(a) (b)

Fig. 9. Comparison of collision traces (**a**. accident vehicle trace; **b**. simulating collision trace)

Considering the e-Bike rider's injuries in the accident, the biomechanical parameters of the ribs and lungs were used as a reference, as shown in Figure 10. The strain of the ribs reaches a peak (4.6%) at around 60ms, and the maximum stress in the lungs appears at around 50ms (203kPa). Further details are provided in the Appendix.

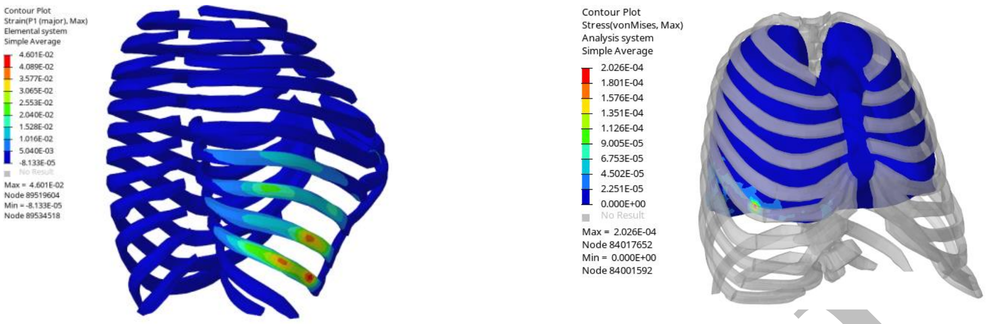

max Strain=4.6% @58ms (a)

max Stress=203kPa @50ms (b)

Fig. 10. Thorax injury situation (**a**. Rib Strain; **b**. Lung Stress)

The maximum rib deflection occurred at the 8th rib, with a deflection of 41.9mm at 74ms, as shown in Figure 11.The maximum deflection at the outermost point of the ribs was observed at the 9th rib, also at 74ms, with the deflection of 33.1mm, as depicted in Figure 12.

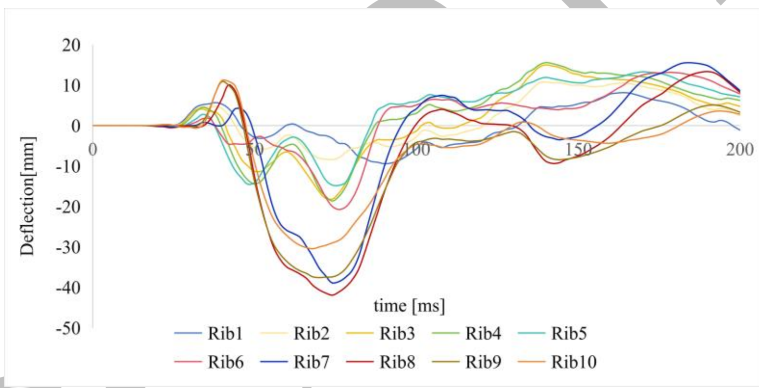

Fig. 11. THUMS maximum rib deflection (mm)

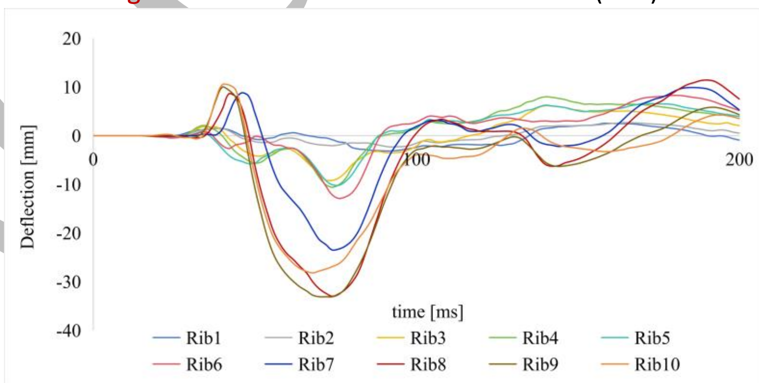

Fig. 12. THUMS rib outermost deflection

Thorax Response Comparison

The whole-body motion of the e-Bike rider and the motion of the WorldSID thorax module within 90ms are contrasted in Figure 13 and Figure 14, the WorldSID thorax module without added abdominal mass reaches its compression peak around 60 ms, while the WorldSID thorax module with added abdominal mass reaches its compression peak around 70 ms.

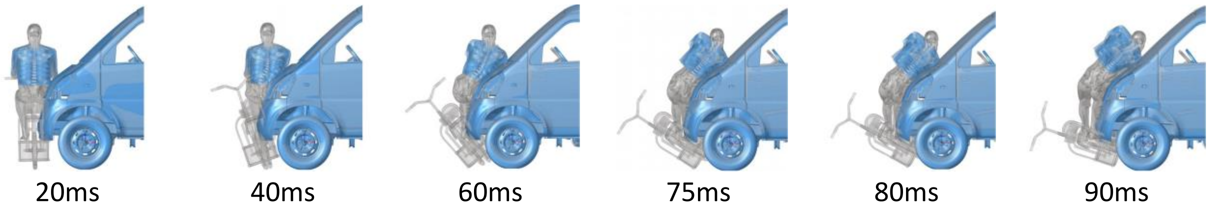

Fig. 13. Comparison of WorldSID thorax module and THUMS Motion (Without the added abdominal mass)

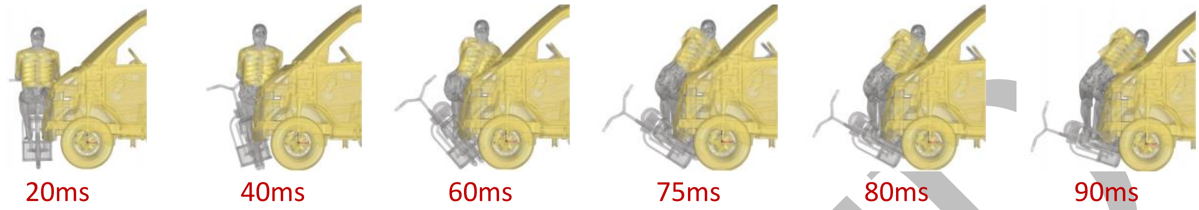

Fig. 14. Comparison of WorldSID thorax module and THUMS Motion (With the added abdominal mass)

The deflection of the three WorldSID thorax module ribs was output, as shown in Figure 15. For the WorldSID thorax module without added abdominal mass (Figure 15.a), the maximum deflection peak (27.9mm) is observed at the third rib, which occurs at a time of 57ms, it can also be observed that the peak value of the deflection for the second rib is 17.2mm, which occurs at 63ms, and for the first rib, the peak value of deflection is 16.0mm, which occurs at 62ms. For the WorldSID thorax module with added abdominal mass (Figure 15.b), the maximum deflection peak (45.6mm) is observed at the third rib at 67ms; a deflection peak of 37.4mm is observed at the second rib at 69ms; and a deflection peak of 37.0mm is observed at the first rib at 70ms.

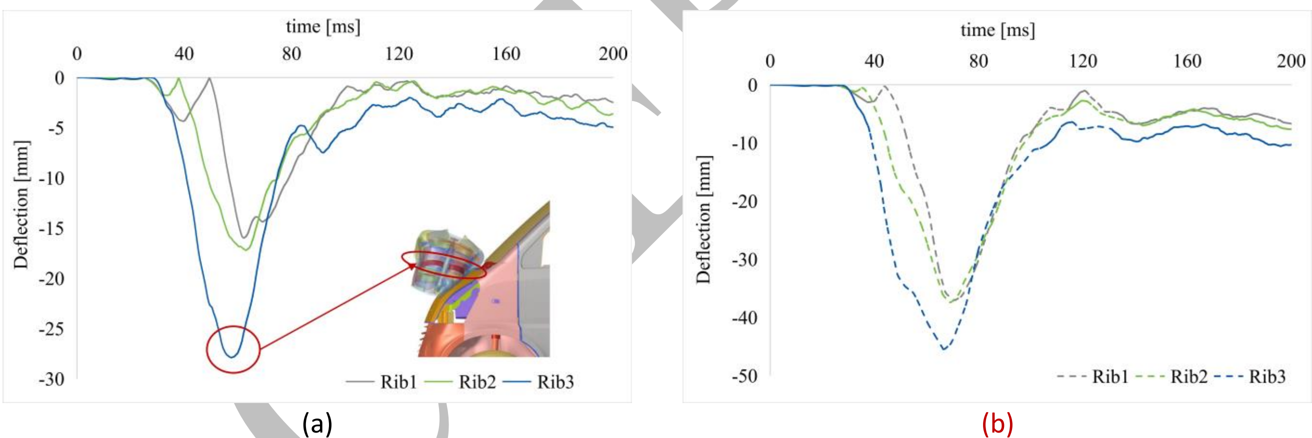

Fig. 15. WorldSID rib deflection(**a**. Without the added abdominal mass; **b**. With the added abdominal mass)

The measurement points for the WorldSID thorax module deflection are relatively close to the measurement points for the outermost ribs six to eight of the THUMS, as shown in Figure 16, with the measurement differences as shown in Figure 17.

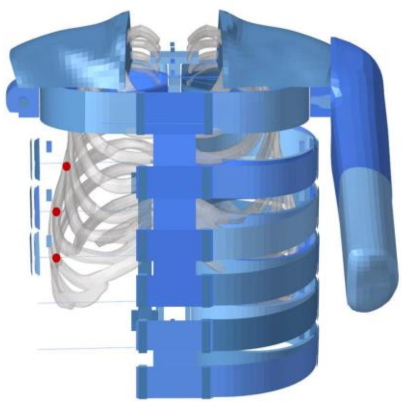
Fig. 16. Comparison of WorldSID thorax module measurement points and THUMS rib deflection

measurement points

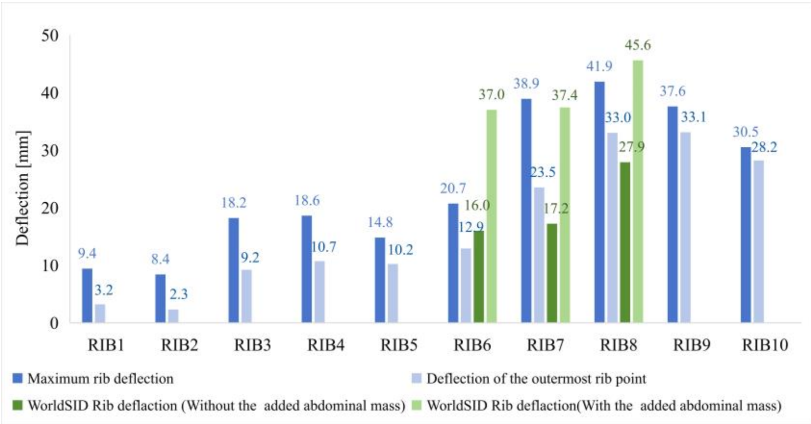

Fig. 17. Peak rib deflection values of THUMS and WorldSID

IV. DISCUSSION

Upon comparison of the minivan-to-eBike accident video and the reconstructed animation, the human motion process of the accident reconstruction is largely consistent with the actual accident process. The e-Bike rider's leg, hip, thorax, and head made contact with the minivan in succession, and the time was close to that of the accident. Examining the collision traces on the vehicle, there are distinct impact marks on the left side of the vehicle's windshield, hood, and bumper, which align with the simulated vehicle traces. By combining the accident video with the simulation animation, it can be determined that these marks were caused by the e-Bike rider's head, thorax, and e-Bike, respectively, and that the deformation on the lower right of the simulated vehicle was due to the e-Bike. From the video, it can be seen that the e-Bike rider began to rotate 160ms later, compared to the simulation results, the e-Bike rider's rotation is more obvious in the video, which may be because the simulation did not take into account the deceleration of the e-Bike. However, the purpose of the reconstruction is to obtain the maximum deflection of the human thorax in the X direction during the accident for comparison with the deflection of the WorldSID thorax module, and this value appears before 80 ms. At this time, the VRU does not show obvious rotation. Therefore, the motion after 160ms is not discussed. Figure 10 shows the cloud map of internal organ and rib injuries, where the right lung stress reaches 203kPa, far exceeding the threshold for lung contusion (±10kPa) [14], consistent with the condition of the e-Bike driver's lung contusion. The strain on the right eighth, nineth and 10th rib also greatly exceeds the injury threshold for rib fracture (1.5%) [22], matching the e-Bike rider's multiple rib fractures on the right side. Based on the strain of each rib in the appendix, the method by Forman et al. [5] was used to calculate the overall injury risk to the ribs (66 years old), resulting in a 100% injury risk for AIS2, which consistent with the injury severity level of AIS2 for the e-Bike rider's ribs.Therefore, this accident reconstruction was able to effectively recreate the e-Bike rider's dynamics and thorax injuries during the accident. However, due to the lack of detailed injury information from FASS, a more detailed comparison of injury locations could not be investigated.

From the perspective of the maximum rib deflection and the outermost rib deflection of the THUMS thorax, the deflection of the lower ribs (ribs -10) is significantly larger than that of the upper ribs (ribs 1-5), and the deflection peaks around 75ms. It is observed that there is a significant difference between the maximum deflection and the outermost rib deflection of some ribs, but the peak of the outermost rib deflection is always lower than that of the maximum rib deflection. This indicates that in this VRU collision with the minivan, the maximum deflection of the ribs did not occur at the outermost part of the ribs but rather at the diagonal front of the thorax. Even though no significant rotation of the e-Bike rider's thorax was observed in this simulation, this could be related to the fact that the costal cartilage at the connection between the ribs and the sternum is more prone to deformation, making the ribs near the cartilage more susceptible to deformation. Although the ribs with the largest deformation (ribs seven, eight, and nine) are close to the ribs with the highest strain concentration (ribs eight, nine and 10), the 10th rib with the highest strain is not the rib with the largest deflection. Therefore, when analysing and evaluating rib injury, one cannot simply equate the rib with the largest deflection to the rib with the highest strain value.

When comparing the thorax motion of the WorldSID thorax module with that of THUMS, both are in great agreement when in a compressed state (within 60ms), but the WorldSID rebounds faster than THUMS during the rebound phase, and the difference in movement state gradually increases after 90ms. The reason for this presumably is the influence of the head and neck and lower limbs. From the perspective of WorldSID thorax deflection, it reaches a peak between 55-65ms, about 10ms earlier than the peak of the THUMS thorax deflection,and reaches a peak between 65-70ms after adding abdominal mass. Comparing the movements of WorldSID thorax modules with and without added abdominal mass, the movements of the former are closer to those of THUMS, including the moment of peak deflection is closer and the rebound speed is significantly slower.But the e-Bike rider's spine will show a remarkable bend during the collision, but since the WorldSID thorax module does not have components that can simulate the bending of the human spine, this process cannot be replicated. It can be seen from Figure 17 that the third rib on the right side of the WorldSID thorax module has a large deflection in both simulations, with peak values of 27.9 mm and 45.6mm respectively, which are similar to the positions of the three ribs with the maximum deformation in THUMS (ribs seven, eight and nine), indicating that the deflection peaks of the WorldSID thorax module and THUMS thorax appear in similar positions, WorldSID thorax module showing some predictability for areas with a higher risk of rib fracture. In this paper, the three measurement points of WorldSID thorax deflection are close to the position of the outermost deflection measurement points of the sixth to eighth ribs of THUMS. According to the deflection values of the two (Figure 17), the thorax module of WorldSID without added the abdominal mass has a significant difference compared with the maximum rib deflection of THUMS. After added the abdominal mass, the deflection is significantly increased, which is generally closer to the maximum rib deflection of THUMS. In conclusion, considering abdominal mass is conducive to improving the similarity of thorax response between WorldSID thorax module and THUMS, both in terms of thorax motion and rib deflection.

V. CONCLUSION

In this study, the accident reconstruction was simulated by an FE model based on a real accident case from the FASS accident database. The results indicate that the THUMS motion process, collision points, and thorax injuries are very close to the real records. In the minivan-eBike collision, the WorldSID thorax module can effectively replicate the human thorax motion process during the compression phase. It can also reflect the THUMS rib deflection in the area which is close to the measurement position of its thorax deflection, thereby potentially representing the e-Bike rider's thorax injury condition. The similarity between the WorldSID thorax module and the THUMS thorax response is further improved by adding abdominal mass. However, it cannot replicate the bending of the e-Bike rider's spine during the impact, and the standalone thorax module also lacks the influence of forces from the head, neck and lower limbs. Therefore, to predict the thorax injury condition of e-Bike riders using the WorldSID thorax module, it is necessary to consider the influence of the abdomen and many other factors. Further research is required on its applicability in different vehicle types in combination with more accident data.

Abcdefghijklmnopqrstuvwxyz

VI. REFERENCES

[1] Annual Statistical Report of Road Traffic Accidents of the People's Republic of China.Traffic Management Bureau of the Ministry of Public Security, 2020.

[2] Cavanaugh, J. M., Walilko, T. J., Malhotra, A. *et al.* Biomechanical Response and Injury Tolerance of the Thorax in Twelve Sled Side Impacts. Proceedings of the 34th Stapp Car Crash Conference, 1990, pp.23-38.

[3]Cheng, K., Cui, S., Zheng, M., et al. Study on AEB Testing for Passenger Cars Rear-Ending Trucks Based on Accident Data Mining and Analysis. Chinese Journal of Automotive Engineering, 2024, 14(3):395-403.

[4] Chang, Y., Shi L., Cheng K., *et al.* Research on the Characteristics of Pedestrian Head Injuries Based on In-Depth Investigation of Traffic Accident Data. Chinese Journal of Automotive Engineering, 2024, **14**(03):455-462.

[5]Forman, J., Kulkarni,S., Perez-Rapela,D.,et al. A Method for Thoracic Injury Risk Function Development for Human Body Models. Proceedings of the IRCOBI Conference, 2022, Porto, Portugal.

[6] Fredriksson R., Flink E., Boström O., Backman K. Injury mitigation in SUV-to-pedestrian impacts. Proceedings of the 20th International Technical Conference on the Enhanced Safety of Vehicles (ESV), 2007, Paper No. 07-0308.

[7] Han, Y., Yang, J., Mizuno, K. A Study on the Dynamic Responses and Injury Mechanism of Human Chest in Vehicle-pedestrian Collisions. Automotive Engineering, 2015, **37**(5): p5.

[8] John, J., Klug, C., Kranjec, M., *et al.* Hello, world! VIVA+: A human body model lineup to evaluate sex-differences in crash protection. Frontiers in bioengineering and biotechnology, 2022, 10(918904).

[9] Karadeniz, S. Design, analysis and experimental study of a novel side thorax impactor to be used in pedestrian protection tests for flat front vehicles. Dissertation, 2021, Middle East Technical University.

[10] Li, G., Lyons, M., Otte, D., *et al.* The influence of passenger car front shape on pedestrian injury risk observed from German in-depth accident data. Accident Analysis & Prevention, 2017, **101**: pp.11–21.

[11] Li, G., Tan, Z., Lv, X., *et al.* Numerical Reconstruction of Injuries in a Real World Minivan-to-Pedestrian Collision. Acta Bioeng Biomech, 2019, **21**(2): 21–30.

[12]Liu, N., Shi L., Cui S., Effect of Riding Posture on Femur Injury of Cyclist in Bicycle and Automobile Accident. AUTO TIME, 2024, (14).

[13]Mcconville J T., Clauser C E., Churchill T D.,et al. Anthropometric relationships of body and body segment moments of inertia. anthropometric relationships of body & body segment moments of inertia, 1980. DOI:10.21236/ada097238.

[14] Melvin, J. W., Stalnaker, R. L., Roberts, V. L. *et al.* Impact Injury Mechanisms in Abdominal Organ, Proc. 17*th* Stapp Car Crash Conference, 1973, pp. 115-126.

[15] Staack, H., Labenski, V. Comparison of Chinese and German in-depth accident data of pedestrian thorax and head injuries. Proceedings of the 67th Stapp Car Crash Conference, 2023.

[16] Shigeta, K., Kitagawa, Y., Yasuki, T. Development of Next Generation Human FE Model capable of Organ Injury Prediction. Proceedings of the 21st Annual Enhanced Safety of Vehicles, 2009, Stuttgart (Germany).

[17] Trube, N., Matt, P., Jenerowicz, M. Plausibility Assessment of Numerical Cyclist to Vehicle Collision Simulations based on Acident Data. Proceedings of the IRCOBI Conference, 2023, Cambridge, United Kingdom.

[18] Untaroiu, C. D., Pak, W.; Meng, Y., *et al.* A Finite Element Model of a Midsize Male for Simulating Pedestrian Accidents. Journal of Biomechanical Engineering, 2017, **140**(1).

[19] Wang, F. Development of a Human Thoracic FE Model and Applied Research on Thorax Injury Biomechanics in Vehicle Impact. Dissertation, 2014, Hunan University.

[20] World Health Organization, Global status report on road safety , 2023.

[21] Wisch, M., Lerner, M., Vukovic, E., *et al.* Road traffic crashes in Europe involving older car occupants, older pedestrians or cyclists in crashes with passenger cars: Results from SENIORS. Proceedings of the 25th International Technical Conference on the Enhanced Safety of Vehicles (ESV), 2017, Paper No. 17-0398.

[22] Wu, T., Kim, T., Bollapragad, V. *et al.* Evaluation of biofidelity of THUMS pedestrian model under a whole-body impact conditions with a generic sedan buck. Traffic injury prevention, 2017, **18**(sup1): S148-S154.

[23] Yang, J. Review of injury biomechanics in car-pedestrian collisions. International Journal of Vehicle Safety, 2005, **1**(3): pp.100–117.

[24] Yamaguchi, R., Makino, Y., Chiba, F. *et al.* Frequency and Influencing Factors of Cardiopulmonary Resuscitation-Related Injuries During Implementation of the American Heart Association 2010 Guidelines: A Retrospective Study Based on Autopsy and Postmortem Computed Tomography. Int. J. Legal Med.,2017, **131**(6): pp.1655-1663.

[25] Zander, O., Ott, J., Wisch, M., *et al.* Safety Enhanced Innovations for Older Road Users (Seniors): Further Development of Test and Assessment Procedures Towards an Improved Passive Protection of Pedestrians and Cyclists. Proceedings of the 25th International Technical Conference on the Enhanced Safety of Vehicles (ESV), 2017, Paper No. 17-0268.

[26] Zander, O., Wisch, M., Ott, J. *et al.* Development and Evaluation of a Thorax Injury Prediction Tool (TIPT) and Possibilities for Incorporation Within Improved Test and Assessment Procedures - Results From Seniors. Proceedings of the 26th International Technical Conference on the Enhanced Safety of Vehicles (ESV), 2019, Paper No. 19-0014.

VII. APPENDIX

TABLE A-I
THE STRAIN OF THE RIBS

Rib1	Rib2	Rib3	Rib4	Rib5	Rib6
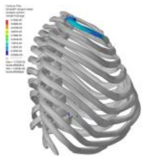	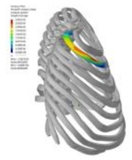	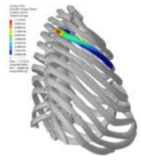	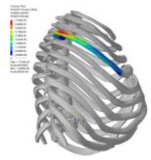	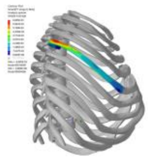	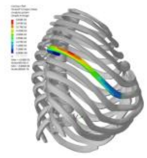
max Strain=0.57% @74ms	max Strain=0.30% @97ms	max Strain=1.12% @94ms	max Strain=0.77% @74ms	max Strain=0.67% @74ms	max Strain=0.67% @70ms
Rib7	Rib8	Rib9	Rib10	Rib11	Rib12
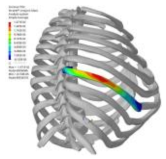	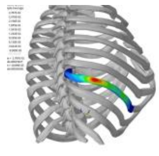	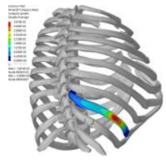	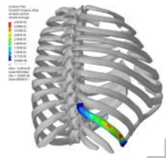	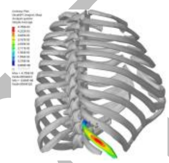	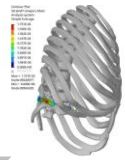
max Strain=1.47% @64ms	max Strain=2.79% @64ms	max Strain=3.82% @60ms	max Strain=4.60% @58ms	max Strain=0.48% @58ms	max Strain=0.18% @48ms